01,11

# On the thermal stability of nanostructure due to microalloying with interstitial elements: Fe-Cr-N nanocrystalline system

© G.A. Dorofeev, A.L. Ulyanov, V.E. Porsev

Udmurt Federal Research Center, Ural Branch Russian Academy of Sciences,
Izhevsk, Russia

E-mail: gadorofeev@udman.ru

*Received June 12, 2023*
*Revised September 12, 2023*
*Accepted September 13, 2023*

Low thermal stability of grain structure is the main factor preventing the use of nanocrystalline (NC) materials at elevated temperatures. In this paper, a comparative study of the thermal stability of NC grain sizes of pure $\alpha$-Fe and Fe-20Cr, Fe-19.5Cr-0.5N (at.%) ferritic alloys obtained by mechanical alloying was carried out. It has been shown that the Fe-20Cr binary alloy is much more thermally stable than NC $\alpha$-Fe. However, the Fe-19.5Cr-0.5N NC alloy does not show a strong increase in thermal stability compared to Fe-20Cr, despite the fact that $Cr_2N$ particles are precipitated during the heating process. It is shown that the actual size of $Cr_2N$ particles (30 nm according to the broadening of X-ray diffraction peaks) significantly exceeds the critical particle size $d^* = 8$ nm above which, according to Gladman, there is no pinning of grain boundaries. Effective strategies for increasing the thermal stability of nitrogen microdoped Fe-Cr alloys are discussed within the critical size model of pinning particles and the thermokinetic grain growth model.

**Keywords:** mechanical alloying, nanocrystalline Fe-Cr alloy, nitrogen, thermal stability.

DOI: 10.61011/PSS.2023.11.57308.105

## 1. Introduction

According to the Hall–Petch law, as the grain size of polycrystalline alloys decreases, their strength increases [1]. At the same time, in the range of nanocrystalline (NC) grains (grain size less than 100 nm), the plastic properties of alloys often behave unusually: instead of the typical inverse strength-plasticity relationship, nanocrystalline alloys demonstrate high plasticity at high strength. Therefore, in recent decades there has been a trend in the development of methods for producing NC materials and their use as substitutes for conventional polycrystalline materials. However, despite all the advantages in properties, due to the strong nonequilibrium of nanograin boundaries and their high density, NC materials have a significant drawback, which is the low thermal resistance to grain growth [2–9]. Grain growth results in degradation of properties and narrows the temperature range of application of NC materials. Therefore, stabilization of grain sizes is an urgent problem in the field of NC materials and their applications.

In the scientific literature of recent years, two approaches (mechanisms) have been outlined for increasing the thermal stability of NC materials: thermodynamic and kinetic approaches [2–9]. From the energy-based point of view, nanograin boundaries make the main contribution to the increased free energy of the alloy. Therefore, factors that reduce the boundary energy should lead to stabilization of the grain structure. The thermodynamic stabilization can be achieved by solute segregation at the grain boundaries if this segregation leads to a decrease in the boundary energy. On the other hand, due to the fact that the grain growth occurs by migration of boundaries, in order to inhibit the grain growth it is necessary to create an obstacle to the movement of boundaries and thereby increase the activation energy of the grain growth. The kinetic stabilization takes place when a moving grain boundary encounters obstacles such as dispersed second-phase particles (Zener pinning) [10,11]). A typical technique for increasing the thermal stability of NC materials is the creation of segregations of impurity atoms at the grain boundaries. Grain boundary segregations (GBS) can provide a synergetic combination of these two approaches: GBS reduce the boundary energy and thus reduce the thermodynamic driving force for the grain growth; GBS restrain the migration of boundaries by securing them [10–12]. It should be noted that the grain thermal growth inhibitory effect has been studied experimentally and using theoretical modeling quite well only for substitutional impurities. The problem of interstitial impurity effect on the grain growth has not been studied both experimentally and theoretically.

Binary body-centered cubic (BCC) Fe-Cr alloys form the basis of an important class of structural materials — ferritic stainless steels, which combine good mechanical properties, high corrosion resistance, and resistance to radiation under exposure to neutron irradiation. They are used as structural materials in the nuclear power industry: for the cladding of fuel rods in fast-neutron reactors operating under irradiation conditions and at temperatures of up to 700°C [13,14]. As our studies have shown [15], an intensive grain growth in binary Fe-Cr NC alloys upon heating begins from 500–600°C.

In this study, we have focused on the possibility of thermal stabilization of the nanograin size in the Fe-Cr NC system due to microalloying of a binary alloy with nitrogen. It was assumed that nitrogen could segregate at grain boundaries and form dispersed precipitates of the second phase there and thereby prevent the thermal growth of grains. An effective method for producing alloys with an NC structure is mechanical alloying (MA) in high-energy ball mills. Nitriding of alloys by MA in the nitrogen gas phase is usually a difficult task, because it requires a continuous supply of gas to the mill vessel to maintain the required pressure. In this study, the Fe-Cr alloy was nitrided due to the deformation-induced dissolution of $Cr_2N$ chromium nitride added to the processed powder mixture of Fe and Cr. The effectiveness of this method of mechanical nitriding has been shown in [16].

The purpose of this work was to study the mechanisms of mechanical alloying of $Fe + Cr + Cr_2N$ powder mixture in a high-energy ball planetary mill to produce Fe-Cr-N nanocrystalline alloy with 0.5 at.% N, solid-phase processes during annealing of mechanically alloyed nanocrystalline samples and establishing criteria for the effectiveness of microalloying with interstitial elements as a factor in restraining the grain growth during heating.

## 2. Experiment

In this study, thermal stability of the Fe-19.5Cr-0.5N (at.%) NC alloy was investigated and the results were compared with those for $\alpha$-Fe and Fe-20Cr NCs from previous studies [17] and [15], respectively. Powders of carbonyl iron of ultra high purity grade 13-2 (99.98 wt.% Fe), pure chromium (99.98–99.99 wt.%) and $Cr_2N$ chromium nitride were used as initial materials to prepare mixtures for the MA. Nitrogen is a strong austenite former in steels. Therefore, to maintain the ferritic BCC structure of the alloy, it is necessary to inject less than 1 at.% N. In this study, the powder mixture was taken in proportions ensuring nominal composition of Fe-19.5Cr-0.5N in at.%. MA experiments were performed using a Pulverizette-7 planetary ball mill, in a protective argon atmosphere. Weight of the powder mixture charged into each vessel of the mill was 10 g. Processing time of the mixture in the mill was selected up to 16 h, after which the entire sample was discharged for studying and annealing. Mechanically alloyed samples were isothermally annealed in a vacuum oven at temperatures of up to 700°C with holding for 4 h.

X-ray diffraction studies were performed using a Rigaku Miniflex 600 diffractometer (Bragg–Brentano geometry, $CoK_\alpha$ radiation with a nickel filter). Phases were qualitatively analyzed using the Crystallography Open Database (COD) of phases via QualX2 software [18]. Sizes of crystallites and magnitudes of lattice microdistortions were determined from the analysis of the profile of diffraction lines by fitting them with a Voigt function. It was assumed that the Lorentz width of the Voigt function provides information about the average size of crystallites $\langle L \rangle$, and the Gaussian width provides information about the magnitude of microdistortions $\langle \varepsilon^2 \rangle^{1/2}$ according to the following formulae [19,20]:

$$\langle L \rangle = \frac{\lambda}{\beta_C^{\text{phys}} \cos\theta}; \quad \langle \varepsilon^2 \rangle^{1/2} = \frac{\beta_G^{\text{phys}}}{4 \operatorname{tg}\theta}, \tag{1}$$

where $\lambda$ is X-ray wavelength, $\theta$ is Bragg angle of the line, $\beta_C^{\text{phys}}$ and $\beta_G^{\text{phys}}$ are Lorentz (Cauchy) and Gaussian physical widths of the line in radians of $2\theta$, respectively. Physical widths of lines were determined from experimental ($\beta_C^{\text{exp}}$, $\beta_G^{\text{exp}}$) and instrumental ($\beta_C^{\text{instr}}$, $\beta_G^{\text{instr}}$) widths using the relationships of $\beta_C^{\text{phys}} = \beta_C^{\text{exp}} - \beta_C^{\text{instr}}$ and $\beta_G^{\text{phys}} = \sqrt{(\beta_G^{\text{exp}})^2 - (\beta_G^{\text{instr}})^2}$. The diffraction pattern of $\alpha$-quartz ($\alpha$-$SiO_2$) recorded by the diffractometer under the same imaging conditions as those of the samples was used as a standard (reference) to determine $\beta_C^{\text{instr}}$ and $\beta_G^{\text{instr}}$. The obtained dependences of $\beta_C^{\text{instr}}$ and $\beta_G^{\text{instr}}$ on the angle of $2\theta$ approximated by third-degree polynomials made it possible to take into account the contribution of instrumental broadening for any phases in the sample over the entire range of $2\theta$ angles. Mössbauer spectra were recorded at room temperature in transmission geometry by a SM2201DR Mössbauer spectrometer (with $^{57}Co$ isotope in Rh matrix as a source of $\gamma$-quanta). The spectra were mathematically processed by the method of restoration of distribution functions of hyperfine magnetic fields $P(H)$ from the experimental spectrum [21]. The morphology of powder particles at various MA stages and their elemental composition were studied using a Thermo Fisher Scientific Quattro S scanning electron microscope equipped with an energy dispersion analyzer. Calorimetric measurements (DSC) were carried out using a DSC Netzsch Pegasus 404C differential scanning calorimeter in the argon atmosphere with sample heating at a rate of 10 deg/min.

## 3. Results

### 3.1. Mechanical alloying

The analysis of X-ray diffraction patterns and Mössbauer spectra taken after MA of the $Fe + Cr + Cr_2N$ powder mixture for up to 16 h showed the following. In the diffraction patterns, X-ray reflections of the independent phase of the $Cr_2N$ nitride are present only up to 1 h of MA, after which they disappear. In addition, there is a sharp increase in the lattice parameters of $\alpha$-Fe and $\alpha$-Cr. And the amount of $\alpha$-Fe phase increases, and $\alpha$-Cr decreases. The simultaneous increase in the parameters of $\alpha$-Fe and $\alpha$-Cr means alloying of these phases with nitrogen due to the deformation dissolution of chromium nitride: nitrogen atoms in the metal matrix form an interstitial solid solution, which leads to expansion of the crystal lattice. In other respects the MA mechanism is similar to that for the

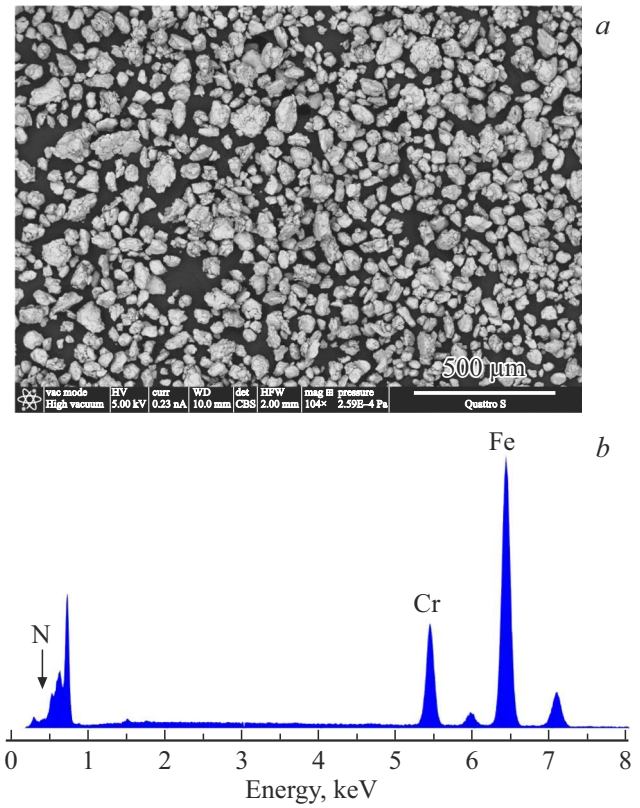


**Figure 1.** *a* — particle morphology and *b* — energy dispersive analysis of the powder after mechanical alloying for 16 h.

Fe-Cr binary alloy, as we have shown in [15]: MA occurs through the preferential diffusion of Cr into Fe. As a result of deformation atomic mixing during the MA for 16 h a single phase is formed: BCC substitution-interstitial solid solution of $\alpha$-Fe(Cr, N). In this case, the width of diffraction lines reaches its maximum; the analysis of broadening shows a crystallite size of $\sim 8$ nm. Figure 1, *a* shows the morphology of powder particles after 16 h of MA, and Figure 1, *b* shows the results of energy-dispersive analysis. The powder particles have an average size of $30-50\,\mu$m, the chemical composition is well consistent with that expected from the ratio of components in the initial powder mixture. Low-energy peaks in Figure 1, *b* (energy less than 1 keV) are indicative of the presence of light elements: nitrogen, carbon, oxygen.

### 3.2. Annealing of mechanically alloyed samples

To study the thermal stability of NC samples after MA, they were isothermally annealed in a vacuum oven in a temperature range of $400-700^\circ$C for 4 h. Figure 2 shows diffraction patterns of samples immediately after MA and subsequent annealing. With $T_{ann} \leq 500^\circ$C, the only phase in the sample is the BCC phase with a lattice constant of 0.2877 nm. Additional reflections in the diffraction pattern appear after annealing at $T_{ann} \geq 600^\circ$C. These reflections are clearly identified as belonging to the $Cr_2N$ nitride phase. Their intensity is low due to the small amount of nitrogen in the alloy. With the appearance of reflections of $Cr_2N$, the lattice constant of the metal BCC matrix decreases down to 0.2874 nm.

Figure 3 shows the Mössbauer spectra and $P(H)$ functions of samples immediately after MA, as well as subsequent annealing. The $Cr_2N$ nitride phase does not contribute to the spectrum, because the Mössbauer probe in this case was an iron isotope; and only iron-containing phases contribute to the spectra. The spectrum is a sextet of magnetic splitting lines, which is typical for BCC ferromagnetic alloys of Fe-Cr. The broad sextet lines reflect the presence of Cr and N atoms near Fe atoms in the BCC lattice of the concentrated solid solution. During annealing, the Mössbauer spectrum undergoes a noticeable transformation (see $P(H)$ functions in Figure 3). The Mössbauer spectra upon annealing of the Fe-20Cr binary NC alloy were studied in detail by us earlier in [15], where the effect of chromium GBS on the spectrum was shown. Based on a comparison of the spectra of annealed Fe-20Cr and Fe-19.5Cr-0.5N alloys, it can be said that when annealing the Fe-19.5Cr-0.5N NC alloy the initially present chromium GBS disappear as $Cr_2N$ is released. Nitrides released along grain boundaries eliminate the chromium GBS.

Figure 4, *a* shows the average grain size $\langle L \rangle$ and the magnitude of lattice microdistortions $\langle \varepsilon^2 \rangle^{1/2}$ as functions of the annealing temperature, obtained from the analysis of

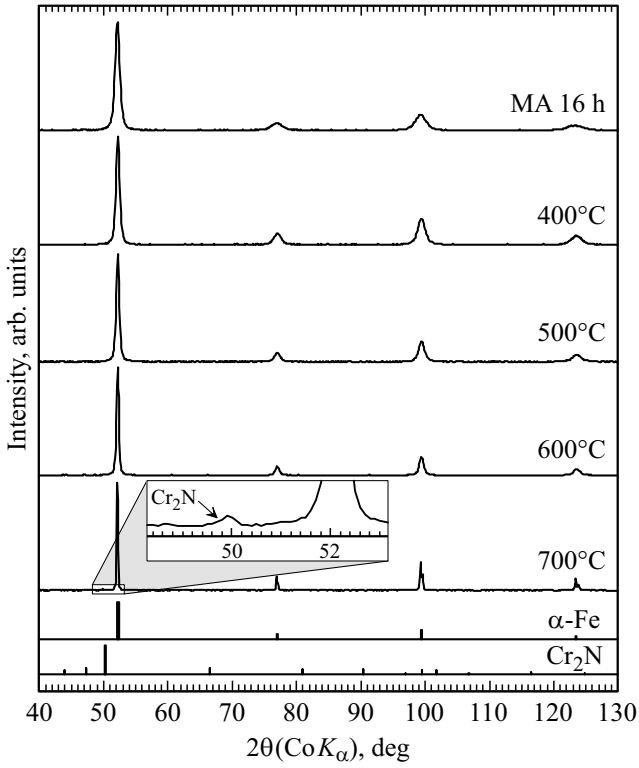


**Figure 2.** X-ray diffraction patterns of powders after mechanical alloying, MA, (16 h) and subsequent annealing at the specified temperatures. Below are line diffraction patterns of the phases.

diffraction patterns of the Fe19.5Cr0.5N sample after MA for 16 h, as well as, for comparison, thermal grain growth for the pure $\alpha$-iron ground in a ball mill to the NC state [17], and mechanically alloyed binary Fe20Cr [15]. It can be immediately observed that Fe20Cr and Fe19.5Cr0.5N NC alloys are much more stable with respect to grain growth than the $\alpha$-Fe NC alloys. The thermal stability of the Fe20Cr alloy is caused by the presence of GBS of Cr, as it was shown in [15]. Microalloying of the Fe20Cr alloy with nitrogen to the composition of Fe19.5Cr0.5N only slightly increases the thermal stability. The beginning of intensive grain growth in the Fe19.5Cr0.5N alloy corresponds to $T_{ann} = 600°C$. Moreover, the decrease in microdistortion begins at lower temperatures. Figure 4, *b* shows the DSC curve when heating the Fe19.5Cr0.5N alloy after MA for 16 h. An intense exothermic peak starting at 600°C corresponds to the release of $Cr_2N$ nitride, which is confirmed by the diffraction patterns in Figure 2. The other two peaks: a sharp peak at 560 and a flat peak at 770°C, are associated with relaxation of defects (dislocations and point defects) and grain growth, respectively. The proof for the origin of two heat release peaks, similar in shape to those observed in our study, for ball-milled $\alpha$-Fe was given in [22]. Indeed, the two above-mentioned heat release peaks in Fe19.5Cr0.5N correlate well in temperature with the changes in $\langle L \rangle$ and $\langle \varepsilon^2 \rangle^{1/2}$ during annealing (see Figure 4, *a*).

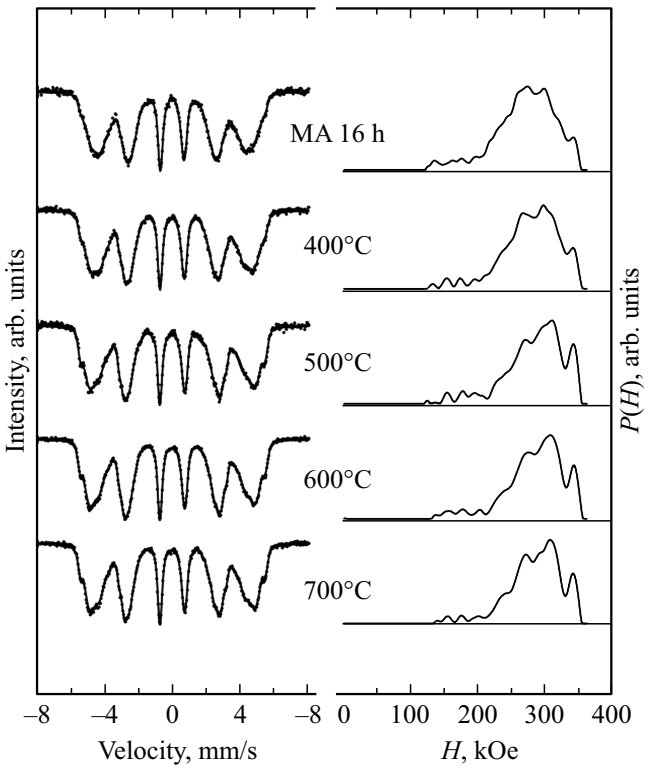


**Figure 3.** Mössbauer spectra (left) and $P(H)$ functions (right) of powders after mechanical alloying, MA, (16 h) and subsequent annealing at the specified temperatures.

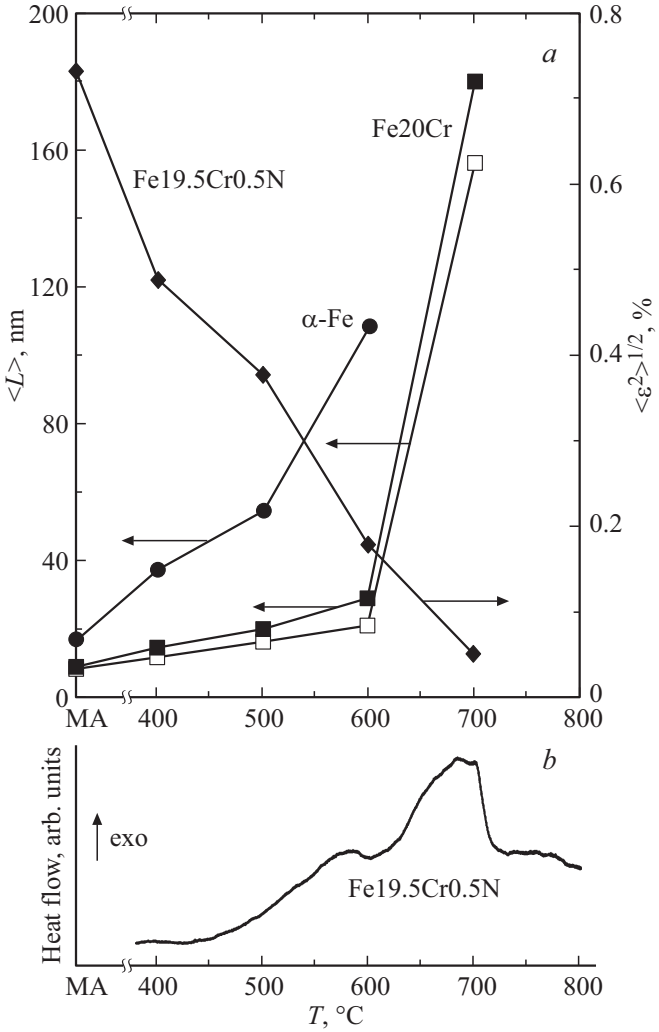


**Figure 4.** *a* — grain sizes $\langle L \rangle$ and microdistortion values $\langle \varepsilon^2 \rangle^{1/2}$ as functions of the annealing temperature for $\alpha$-Fe [17] and Fe20Cr [15], Fe19.5Cr0.5N NC alloys. *b* — DSC curve for the Fe19.5Cr0.5N nanocrystalline alloy.

## 4. Discussion

Thus, high-chromium ferritic steel with microadditives of nitrogen can be produced by MA of iron, chromium and $Cr_2N$ chromium nitride powders. Chromium nitride decomposes under the intense deformation and forms with iron and chromium the NC substitution-interstitial solid solution of $\alpha$-Fe(Cr, N). The NC binary system of Fe20Cr is much more thermally stable with respect to grain growth than NC pure $\alpha$-Fe due to the GBS of Cr formed during heating. Microalloying of the Fe-Cr system with nitrogen does not lead to a significant increase in the thermal stability of the nanostructure compared to the Fe20Cr binary NC alloy. In the process of alloy annealing, precipitation of $Cr_2N$ nitride is observed. However, the nitride particles do not have a significant pinning effect on the matrix grain boundaries, as might be expected. The comparison of BCC phase grain size dependences on the annealing temperature

for the Fe19.5Cr0.5N sample under study and the Fe20Cr sample without nitrogen shows that in both cases the most intensive grain growth begins with an annealing temperature above 600°C. At the annealing temperature of 700°C and higher, in both cases the grain size reaches values above 100 nm. $T_{ann} = 600$°C is the critical temperature above which the intensive grain growth begins.

The idea of grain boundaries pinning by dispersed particles of the second phase was suggested for the first time by Zener [10,11]. Zener came to a simple equation relating the size of spherical grains with a radius of $R$ of the matrix, the radius of spherical particles of the second phase $r$ and the volume fraction of these particles $f$: $R = 4r/3f$. The equation shows that the pinning effect from the second-phase particles is greater (less $R$) the smaller is the size of the pinning particles and the greater is their volume fraction. Subsequently, the equation was refined, but the physical essence of the equation remained unchanged: the dispersed precipitates of the second phase restrain the growth of matrix grains by pinning the boundaries by these particles of precipitates — the Zener pinning. Later, Gladman [23], based on the Zener equation and considering the energy situation when the grain boundary is to overcome an energy barrier being detached from the particles, has found an expression for the critical radius of particles $r^*$:

$$r^* = \frac{6Rf}{\pi}\left(\frac{3}{2} - \frac{2}{Z}\right)^{-1}, \qquad (2)$$

where $Z$ is the heterogeneity factor, that is the ratio of the radii of the growing grain and the neighboring grain. The comparison with experimental data made it possible to establish that $Z$ is between $\sqrt{2}$ and 2, and the actual value is $Z > 1.5$. The critical radius of pinning particles $r^*$ is the particle size above which the grain boundaries of the matrix can easily detach from the particles, that is, the Zener pinning does not work. Therefore, the Zener pinning criterion can be formulated as $r < r^*$. Moreover, according to Gladman, the smaller the initial grain of the matrix, the smaller particles are required to secure its boundaries. In addition, the critical radius of the pinning particles depends on their density (volume fraction): the higher the particle density, the larger the particle size is required for the effective pinning of grain boundaries. The Gladman's model is well consistent with experiment [24].

Let us estimate the critical size of pinning particles (critical diameter $d^* = 2r^*$) for the Fe19.5Cr0.5N system under study. For this purpose, assume $Z = 2$ as the most realistic value for the factor of heterogeneity [24]. Then equation (2) for the critical particle diameter takes the following form: $d^* = 24Rf/\pi$. We will perform the calculation for the annealing temperature at which all $Cr_2N$ particles are released from the solid solution, that is, all the nitrogen has entered into reaction. This case corresponds to $T_{ann} = 700$°C, i.e. the temperature of completion of the heat release associated with $Cr_2N$ (see Figure 4, *b*). For this temperature, we can take $R = 80$ nm as the grain radius of the matrix. By substituting, we get $d^* \approx 8$ nm. The analysis of the line profile of the $Cr_2N$ phase, that appear starting from 500°C (see Figure 2), gives the average particle size of $\langle L\rangle_{Cr_2N} \approx 30$ nm for this phase, i.e. $\langle L\rangle_{Cr_2N} > d^*$. Hence, according to the Gladman's model, the weak effect of nitrogen microalloying on the thermal stability of the Fe-Cr NC alloy is explained by the size of the released particles of $Cr_2N$ when the annealing is larger than the critical one.

There are more recent publications concerning the stability of NC alloys, of which it is worth taking into account, first of all, the studies of Chen et al. [25,26]. Combining thermodynamic and kinetic approaches, they have shown that in nanosystems, in particular in Fe-Cr, where thermal stabilization of the grain size is possible both due to grain-boundary segregations and due to second-phase precipitation, stabilization occurs during annealing in several stages. The first stage is the formation of GBS of the impurity accompanied by a decrease in the energy of the boundaries, and therefore a decrease in the thermodynamic driving force of grain growth (insignificant grain growth and its subsequent stabilization). GBS have a double effect on stabilization: they reduce the energy of boundaries (thermodynamic effect) and secure boundaries from migration (kinetic effect). The second stage is the GBS-based nucleation and growth of second-phase particles accompanied by depletion (resorption) of segregations; the energy of the boundaries increases, and the thermodynamic driving force of grain growth increases. The grains grow intensively; the thermodynamic effect (reduction of boundary energy) from the GBS stabilizes the grains more effectively than the kinetic effect (boundaries pinning) [26]. Thus, if the component in the segregations is the main component of the second phase, there is a competition between the influence of these two factors (GBS and segregation of the second phase) on the grain growth.

In conclusion, we will discuss possible more successful strategies for increasing the thermal stability of Fe-Cr alloys due to GBS and nitride precipitation. In ferrite of chromium steels, $Cr_2N$ particles nucleate heterogeneously within grain boundaries [27]. In the NC alloy, the density of $Cr_2N$ nuclei is high due to the high density of grain boundaries. But particles grow with increasing temperature and are subject to coalescence due to diffusion. According to [28,29], the radius $R$ of second-phase particles increases during the annealing time $t$ according to the equation of $R = \alpha\sqrt{Dt}$, where $D$ is diffusion constant of a dissolved element and $\alpha$ is dimensionless coefficient. It is clear from this that the controlling factor in the growth of $Cr_2N$ particles is the diffusion constant of chromium, which is known [30] to be proportional to the concentration of the main component of the Cr precipitates. Therefore, to slow down particle growth, the chromium content of the ferrite should be reduced. It should be noted that corrosion-resistant ferritic steels for the nuclear power industry usually contain 12−14% of Cr. On the other hand, the critical size of nitride particles can be increased by increasing the volume fraction of nitrides (see equation (2)). To do this, an increase

in the nitrogen content in steel is needed. However, as noted above, due to the strong austenite-forming ability of nitrogen in the Fe-based solid solution, an increase in the nitrogen content at the stage of solid solution formation will lead to the $\alpha$-Fe(Cr, N) $\rightarrow$ $\gamma$-Fe(Cr, N) phase transformation, which transforms steel from ferritic to austenitic class (the investigation of austenitic steels was not the purpose of this study). The next aspect that should be taken into account is the above-mentioned competition between the influence of the GBS and second-phase precipitates on the grain growth [25]. To eliminate this competition in Fe-Cr NC alloys, it is rational to use chromium-free nitride instead of $Cr_2N$. Such a nitride can be TiN or AlN. These nitrides are much more thermodynamically stable than $Cr_2N$ (the enthalpies of formation of $\Delta H_{\text{form}}$ $Cr_2N$, TiN, and AlN are $-105.5$, $-336.3$, and $-320.3$ kJ/mol respectively, see, for example [31]). Hence, by adding about 0.5 at.% of Ti or Al into the alloy, TiN or AlN nitrides should be resulted from the annealing instead of $Cr_2N$. At the same time, the GBS of chromium should be preserved.

## 5. Conclusions

1. In order to study the effect of nitrogen additions (0.5 at.%) in nanocrystalline high-chromium ferritic steel of the Fe-20 at.% Cr composition on its thermal stability relative to nanograin growth, mechanical alloying was carried out in a ball planetary mill of $Fe + Cr + Cr_2N$ powder mixture. Mechanical alloying occurs in several stages, including deformation-induced dissolution of chromium in iron, dissolution of $Cr_2N$ nitride, accompanied by alloying of the BCC solid solution of Fe-Cr with nitrogen. The final product of mechanical alloying is the BCC substitution-interstitial solid solution of $\alpha$-Fe(Cr, N) with a grain size of about 8 nm.

2. According to differential thermal analysis, the heat release peak at 580°C during heating of mechanically alloyed samples is associated with the formation of $Cr_2N$ nitride, which is confirmed by X-ray diffraction after annealing. The stability of the Fe-20 at.% Cr binary nanocrystalline alloy is much higher than that of the pure nanocrystalline $\alpha$-Fe, which is associated with chromium segregations along grain boundaries. Microalloying of the Fe-20 at.% Cr nanocrystalline alloy with nitrogen to the composition of Fe19.5Cr0.5N (in at.%) does not provide a significant increase in thermal stability compared to the Fe-Cr-binary alloy.

3. The actual size of $Cr_2N$ particles (30 nm according to the broadening of diffraction reflections) significantly exceeds the critical particle size of $d^* = 8$ nm, below which, according to Gladman, the pinning of grain boundaries is effective. In addition, as $Cr_2N$ nitride is released, grain-boundary segregations of chromium disappear.

4. Effective strategies for increasing the thermal stability of Fe-Cr alloys microalloyed with nitrogen are discussed within the framework of the critical size model of pinning particles and the thermokinetic model of grain growth. An assumption is made that reducing the Cr content to 10–12%, as in high-grade chromium ferritic steels, will reduce the size of nitride precipitates below the critical size. It is also possible that the introduction of about 0.5% of Ti or Al into the alloy will ensure the replacement of chromium nitride in the alloy with TiN or AlN nitride with maintaining the grain boundary segregations of Cr.

### Funding

The study was carried out using the equipment of the Shared Use Center „Center of Physical and Physicochemical Methods of Analysis and Study of Properties and Characteristics of the Surface, Nanostructures, Materials and Products“ of the Udmurt Federal Research Center of the Ural Branch of RAS within the framework of the state assignment of the Ministry of Science and Higher Education of the Russian Federation (No. of state registration 121030100003-7).

### Conflict of interest

The authors declare that they have no conflict of interest.

## References

[1] E.N. Hahn, M.A. Meyers. Mater. Sci. Eng. A. **646**, 101 (2015).
[2] N. Liang, Y. Zhao. J. Alloys Compd. **938**, 168528 (2023).
[3] R.A. Andrievsky. Uspekhi khimii **71**, 967 (2002). (in Russian).
[4] H.R. Peng, M.M. Gong, Y.Z. Chen, F. Liu. Int. Mater. Rev. **62**, 303 (2017).
[5] H. Peng, Z. Jian, F. Liu. Int. J. Ceram. Eng. Sci. **2**, 49 (2020).
[6] C.E. Krill, H. Ehrhardt, R. Birringer. Int. J. Mater. Res. **96**, 1134 (2022).
[7] J.W. Cahn. Acta Met. **10**, 789 (1962).
[8] M. Hillert, B. Sundman. Acta Met. **24**, 731 (1976).
[9] R.A. Andrievski. J. Mater. Sci. **49**, 1449 (2014).
[10] P.A. Manohar, M. Ferry, T. Chandra. ISIJ Int. **38**, 913 (1998).
[11] K. Huang, R.E. Logé. Zener pinning. Ref. Modul. Mater. Sci. Mater. Eng. (2016). P. 1–8.
[12] A.R. Kalidindi, C.A. Schuh. Acta Mater. **132**, 128 (2017).
[13] R.L. Klueh, D.R. Harries / Ed. R. Klueh, D. Harries. 100 Barr Harbor Drive. PO Box C700. West Conshohocken. PA 19428-2959: ASTM International (2001).
[14] K. Ehrlich K, J. Konys, L. Heikinheimo. J. Nucl. Mater. **327**, 140 (2004).
[15] V.E. Porsev, A.L. Ulyanov, G.A. Dorofeev. Met. Mater. Trans. A **50**, 5977 (2019).
[16] G.A. Dorofeev, I.V. Sapegina, V.I. Ladyanov, B.E. Pushkaryov, E.A. Pechina, D.V. Prokhorov. FMM **113**, 1014 (2012). (in Russian).
[17] C.H. Moelle, H.J. Fecht. Nanostruct. Mater. **6**, 421, (1995).
[18] A. Altomare, N. Corriero, C. Cuocci, A. Falcicchio, A. Moliterni, R. Rizzi. J. Appl. Cryst. **48**, 598 (2015).
[19] T.H. De Keijser, J.I. Langford, E.J. Mittemeijer, A.B.P. Vogels. J. Appl. Crystallogr. **15**, 308 (1982).

[20] G.A. Dorofeev, A.N. Streletsky, I.V. Povstugar, A.V. Protasov, E.P. Elsukov. Kolloid. zhurn. **74**, 710 (2012). (in Russian).
[21] E.V. Voronina, N.V. Ershov N.V, A.L. Ageev, Yu.A. Babanov. Phys. Status Solidi **160**, 625 (1990).
[22] Y.H. Zhao, H.W. Sheng, K. Lu. Acta Mater. **49**, 365 (2001).
[23] T. Gladman. Proc. Royal Soc. London. Ser. A. Mathemat. Phys. Sci. **294**, 298 (1966).
[24] A.K. Koul, F.B. Pickering. Acta Met. **30**, 1303 (1982).
[25] Z. Chen, F. Liu, X.Q. Yang, C.J. Shen, Y.M. Zhao. J. Alloys Compd. **608**, 338 (2014).
[26] Z. Chen, F. Liu, X.Q. Yang, C.J. Shen. Acta Mater. **60**, 4833 (2012).
[27] K.A. Bywater, D.J. Dyson. Met. Sci. **9**, 155 (1975).
[28] A. Deschamps, C.R. Hutchinson. Acta Mater. **220**, 117338 (2021).
[29] C. Zener. J. Appl. Phys. **20**, 950 (1949).
[30] Ya.S. Umansky, Yu.A. Skakov. Fizika metallov. Atomnoe stroenie metallov i splavov, Atomizdat, M., (1978). 352 s. (in Russian).
[31] G.V. Samsonov. Nitridy. Nauk. dumka, Kiev, (1969), 380 s. (in Russiasn).

*Translated by Y.Alekseev*